ORIGINAL ARTICLE

TEKSTİL VE KONFEKSİYON

VOL: 36, NO. 3
DOI: 10.32710/tekstilvekonfeksiyon.1680999



Production and Characterization of Poly Lactic Acid (PLA) Meltblown Nonwovens For Air Filtration

Ege ERTOGRUL [1] 0000-0001-6391-8132
Deniz DURAN KAYA [2] 0000-0002-4745-3192

[1] Graduate School of Natural and Applied Sciences, Ege University, Izmir 35040, Türkiye
[2] Department of Textile Engineering, Faculty of Engineering, Ege University, Izmir 35040, Türkiye

Corresponding Author: Deniz Duran Kaya, deniz.duran@ege.edu.tr

ABSTRACT

This paper focuses on reducing the negative impacts of traditional plastics in the production of meltblown filters by using poly lactic acid (PLA) as an environmental friendly biodegradable polymer. In this study the impacts of collector drum speed, die to collector distance (DCD) and die hole diameter on the basis weight, thickness, air permeability, solidity, fiber diameter, water contact angle, and air filtration characteristics of microfibrous PLA nonwovens prepared by meltblowing were investigated. Statistical analyses was conducted by using SPSS software. PLA meltblowns prepared in this study had an average fiber diameter of 2.17 to 3.11 micrometers. The results have shown that, by tailoring the properties of PLA meltblown, filtration performance can be improved while also reducing the environmental impact. This research provides important insights into the production of sustainable meltblown nonwovens by integrating a biodegradable polymer and focusing on the effect of production parameters on material properties.

ARTICLE HISTORY
Received: 21.04.2025
Accepted: 18.07.2025

KEYWORDS

Meltblown, Microfiber, Nonwoven, Polylactic acid (PLA), Air filtration

1. INTRODUCTION

Melt blowing is a method for producing microfiber nonwovens that employs thermoplastic polymers to thin out the melt filaments using high-velocity air. In the fundamental meltblowing procedure, the polymer is heated to a liquid state in an extruder, forced through die openings, and subsequently subjected to high-speed, hot air streams. The web structure starts to develop during the initial fiber entanglement, and a stable network is created when the fibers make contact with the collector. (1-3). It is a unique single-step process where polymer is extruded into fibers with diameters of 1-5 µm. Filtration is regarded as the primary use of meltblown nonwovens, with disposable medical items, wipes, diapers, and feminine hygiene products following closely behind. Filtration plays a crucial role in safeguarding living beings, resources, machinery, and the ecosystem (1, 4).

Meltblown technology is one of the primary methods for filtration media production because it can produce micro fibrous nonwovens cost effectively in a short time. Due to their high permeability and ability to effectively reject fine particles, meltblowns are widely used in the production of various filter media, including cartridge filters, cleanroom filters, face masks, cabin air filters, and HVAC filters. High-quality filtration products primarily consist of meltblown filter layers made from nano or micro-fibers. The meltblowing technique creates extremely fine synthetic nonwovens from various polymers and offers a good degree of control over fiber structure and morphology, making it well-suited for filtration applications. This method allows for high production rates, and the affordability of these filters contributes to their widespread availability for civilian use. Despite the rapid expansion of meltblown fiber applications over the past thirty years, our understanding of the processing parameters remains limited (4, 5).

Polypropylene (PP) is the most widely used polymer for the production of meltblown webs due to its cost effectiveness and versatility, enabling the manufacture of various products. Additionally, other polymers like polyethylene (PE), poly (ethylene tereph-thalate) (PET), poly (butylene terephthalate) (PBT), polystyrene, polyurethane (PUR), and polyamide (PA) can also be employed to produce melt blown webs. However, the majority of the raw materials utilized in meltblowing are produced from petroleum. In most of the products, polypropylene (PP) is utilized because of its cost effectiveness and exceptional processability (1, 4, 6-9).

Nevertheless, synthetic filters possess certain disadvantages because they are neither biodegradable nor biocompatible when they have completed their life cycle. For instance, it

To cite this article: Ertoğrul E, Duran Kaya D. 2026. Production and characterization of poly lactic acid (pla) meltblown nonwovens for air filtration. *Tekstil ve Konfeksiyon,* 36 (3), 230-245.

generally takes 30 to 40 years for 50% of PET-based materials to degrade at 45–100% relative humidity and a temperature of 20 °C. (10, 11).

As concerns about the environmental impact of petroleum-based polymers increase, there is a growing demand for bio-based polymers with less environmental impact to produce meltblown nonwovens, especially for filters. Poly (lactic acid) (PLA) is a promising bio-based alternative to synthetic plastics due to its good mechanical and thermal properties (4, 12).

PLA, which consists of repeating units of lactic acid, is a polymer classified as an aliphatic polyester. A key feature of PLA is its biodegradability and compostability; it is a thermoplastic polymer derived from renewable, starch-rich plant sources like corn, sugar cane, and wheat (13).

Advancements in engineering of PLA, decreasing prices, and an increasing demand for environmental friendly products have supported the application of PLA in various fields such as agriculture, filtration and more (4, 14).

Extensive studies have been conducted on the fabrication and performance of PP meltblown filter media; however, limited research is available on the production of PLA using meltblowing and the impact of material and processing parameters on nonwoven structures and filtration performance. Thus, it is essential to comprehend the properties of PLA polymers in the meltblowing process and the way it impacts structures in the development of PLA filter media.

Hammonds et. al. (15) successfully prepared PLA micro fibrous webs by using low molecular weight PLA and a laboratory type meltblown machinery with a specially designed micro/nano die. The die type, airflow, and distance from the die to the collector (DCD) were identified as variable parameters. They found that the pore size ranged from 1.82 to 10.48 micrometers for the micro fibrous web and from 452 to 818 nanometers for the nano fibrous web.

Zhu et al. (16) prepared PLA/aminated halloysite nanotubes (PLA/A-HNTs) using masterbatches of PLA/A-HNTs that were compatibilized with dual-monomer glycidyl methacrylate-styrene (St-co-GMA) melt-grafted PLA (PLA-g-(St-co-GMA)) to improve the properties of PLA meltblown surfaces. They analyzed the morphology, crystallization, pore size distribution, filtration efficiency, and mechanical properties of the PLA/PLA-g-(St-co-GMA)/-HNT meltblown materials. They reported that the average diameter and pore size of PLA was slightly increased.

Jafari et. al. (4) produced PLA electret filters using the Reicofil meltblown process and compared their filtration efficiencies with PP meltblown filters for 0.3 μm monodisperse DOP (dioctyl phthalate) particles. Their study revealed that the filtration efficiency of un-charged PLA meltblown filters ranged between 15-41%, whereas 80-95% filtration efficiency was obtained with the charged PLA meltblowns. They concluded that Corona charging significantly improved the filtration performance PLA meltblowns. Meltblowns made from PLA and PP displayed similar performance.

Liu et. al. (5) successfully prepared PLA meltblown nonwovens with high strength and toughness based on hierarchical control of microfiber formation. They stated that, filtration efficiency of corona electret PLA meltblown nonwovens was as high as 92.6%, and the pressure drop was 12.3 Pa.

Despite the existing research on PLA nonwovens, there still remains a gap in comprehending the effects of polymer properties and process parameters on nonwoven characteristics and overall filtration efficiency. This study seeks to address this gap by systematically analyzing the influence of meltblown process parameters on the properties of PLA nonwovens.

In this study, effects of production parameters on formation of PLA meltblown filters in an industrial equipment was investigated. The results were compared with those of PP for two samples, produced by using the same production parameters as the PLA samples. For this purpose, commercially available PLA and PP polymers and a Biax meltblown machine was utilized. The effects of production parameters on micro fibrous meltblown nonwovens and their filtration efficiency were evaluated.

2. MATERIAL AND METHOD

2.1 Material

The PLA used in the manufacturing process was InegoTM biopolymer 6252D, featuring a melt index of 70-85 g/10 min at 210°C and a density of 1.24 g/cm³. PLA was purchased from the Natureworks VR. PLA resins were dried at 80°C for 4 hours prior to processing to eliminate moisture. The PP used in the production was from Exxon, with a melt index of 1100 g/10 min at 230°C and a density of 0.09 g/cm³.

2.2 Method

2.2.1 Production of Meltblown Nonwovens

Meltblown nonwovens were produced by using Biax Fiberfilm Meltblown machine with traditional Exxon die system. Graphical illustration of the meltblown machine used in this study is presented in Figure 1.

The basic principle of nonwoven production by meltblown method is presented schematically in Figure 2. According to this method, a thermoplastic fiber-forming polymer is heated to its melting point in an extruder, pushed through die openings, and subsequently exposed to high-speed hot air streams. The streams of hot air that exit from both sides of the die nosepiece quickly stretch the extruded polymer into very fine filaments. These filaments are then propelled by high-velocity air onto a collector screen, resulting in the creation of a finely filtered, self-bonded nonwoven web. The web structure starts to form when the fibers first become entangled; however, the network structure is stabilized only when the fibers make contact with the collector and their movement stops (2, 3, 17).

CC BY NC ND

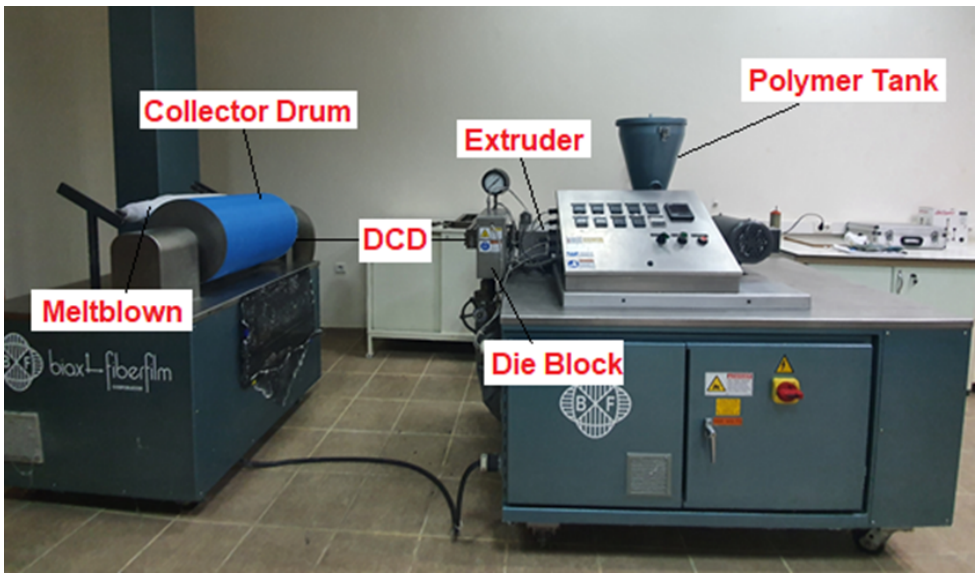


Figure 1. Graphical illustration of the meltblown machine used for the production of nonwovens

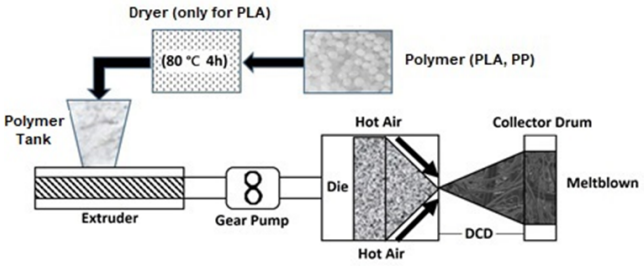


Figure 2. Schematic description of meltblown nonwoven production

PLA and PP polymers were extruded using a single-screw extruder. The meltblowing process was carried out without any additives or stabilizers for both of the polymers. Machine settings used in the meltblowing are given in Table 1.

Production of PLA nonwovens were performed by changing the die hole diameter, collector drum speed and die to collector distance (DCD) parameters. 2 PP samples were also produced with the same production parameters as PLA samples for comparison with PLA nonwovens. Production parameters of the nonwoven samples are shown in Table 2.

Table 1. Main machine settings used in the manufacturing process of meltblown nonwovens

Machine setting	Value for PLA	Value for PP
Air Temperature (°C)	160	193.3
Air Pressure (Psi)	8	8
Extruder Zone 3 Temperature (°C)	210	204.4
Extruder Zone 2 Temperature (°C)	165.5	176.7
Extruder Zone 1 Temperature (°C)	132.2	148.9
Die Metal Temperature (°C)	237.8	185
Extruder Pressure (Psi)	420	394

2.2.3 Characterization of PLA Meltblown Nonwovens

In this study, basis weight, solidity, thickness, air permeability, average fiber diameter (AFD) and fiber diameter distribution, water contact angle (WCA) and air filtration properties of PLA meltblown nonwovens were tested and effects of collector drum speed, die-to-collector distance and die hole diameter were investigated. SEM images of the nonwovens were also taken.

Table 2. Production parameters of the nonwoven samples

Sample Name	Collector Drum Speed (m/min)	Die-to-Collector Distance (DCD) (cm)	Die Hole Diameter (mm)	Polymer
PP-1-50-12	12	50	0.18	PP
PP-1-50-18	18	50	0.18	PP
PLA-1-50-12	12	50	0.18	PLA
PLA-1-50-18	18	50	0.18	PLA
PLA-1-75-12	12	75	0.18	PLA
PLA-1-100-12	12	100	0.18	PLA
PLA-2-50-12	12	50	0.23	PLA
PLA-2-50-18	18	50	0.23	PLA

CC BY NC ND

SEM and Fiber Diameter

The structure and average fiber diameter (AFD) of the micro fibrous webs were examined using a Quanta 2550 FEG electron microscope (SEM) set to an accelerating voltage of 12 kV. To minimize charging effects, the PLA microfiber samples were coated with a fine layer of gold prior to the imaging process. After that, ImageJ software was employed to measure the diameters of the fibers from the SEM images. During the fiber diameter determination, 160 random measurements were taken from 5 images for each sample and thus the AFD was calculated.

Basis Weight, Thickness and Solidity

The basis weight was determined in accordance with the TS EN 29073–1 standard. Measurements were conducted by weighing three specimens, each with an area of 100 cm², and the averages were then computed from these values. The thickness was assessed using the SDL Thickness Gauge in accordance with the TS 7128 EN ISO 5084 standard, employing a presser foot with a diameter of 20 cm² and a weight of 200 g.

The solidity, often referred to as packing density or volume fraction, of the micro fibrous webs was determined using the following equation, which incorporates the measured basis weight and thickness: (4, 18)

$$S = (\text{Basis Weight})/(\text{Thickness} \times \rho)$$

where; S represents solidity, and ρ denotes the density of the polymer (with PLA having a density of 1.24 g/cm³).

Air Permeability

Air Permeability evaluation of the micro fibrous webs was conducted using the FX 3300 Air Permeability testing device, in accordance with the TS 391 EN ISO 9237 standard. The tests were carried out over a measurement area of 20 cm² with a consistent applied air pressure of 100 Pa.

Water Contact Angle (WCA)

KSV Contact Angle Measurement System was used to determine the surface hydrophobicity/hydrophilicity of PLA micro fibrous nonwovens. During the test, pure water of 5l at 21± 3 ℃ temperature has been dropped 14 times onto 1x1 cm sized samples. Picture of each drop was taken during 10 sec. with 1 sec. intervals. Thus contact angle (θ) of the micro fibrous web against the drop on the was measured.

Air Filtration

Filtration performance of the webs were tested according to EN779 test standard. Filtration efficiency (η) and pressure drop (ΔP) of the samples were measured by an automated air filter tester (8130A model, TSI Inc.). The filtration performance evaluation took place with the help of a neutralized, polydisperse sodium chloride (NaCl) aerosol. A 2 wt% NaCl-water solution was used for generating the aerosol particles. The count median diameter of the particles was 0.3 μm. The flow rate of NaCl aerosol was 95 L/min.

During the preparation of aerosol, NaCl solution is nebulized to produce an aerosol laden flow. This flow is conditioned to control the aerosol characteristics, using a heater to isolate particles from the nebulizer water droplets and particle neutralization. The aerosol then passes through the test section, composed of an upstream detector, to measure the particles in the air ahead of the filter; a sample holder, and a downstream detector, to measure the particles after the filter. Photometers are used as detectors, which measure the scattering from an ensemble of particles. The aerosol particles were fed with a face velocity of 15.8 cm/s through the micro fibrous filters with 100 cm^2 test area (10, 19, 20).

The effectiveness of a filter is characterized in means of filtration efficiency (η), pressure drop (P) and quality factor (QF) which combines filtration efficiency and pressure drop (10, 21).

The quality factor (QF) was calculated according to the following equation: (10)

$$QF = -(\ln(1-\eta))/\Delta P$$

where η is the filtration efficiency and ΔP is the pressure drop across the filter (22, 23).

2.2.4 Statistical Analysis

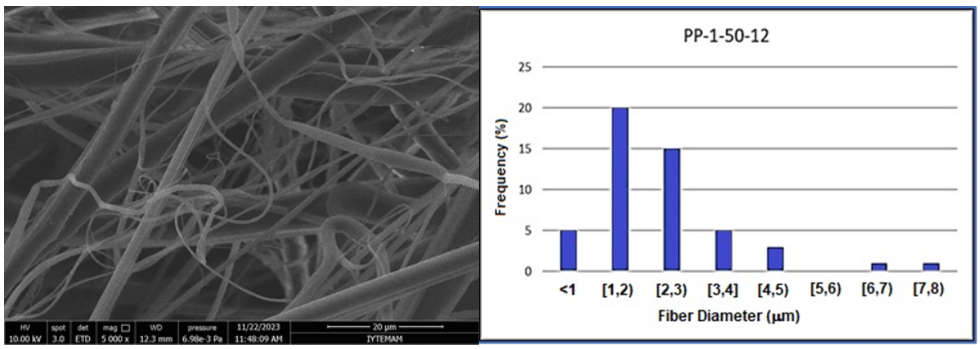
Statistical analysis was conducted by using SPSS software. P-Values less than 0.05 denote statistical significance according to a one-way analysis of variance (ANOVA) in 95% confidence interval.

3. RESULTS AND DISCUSSION

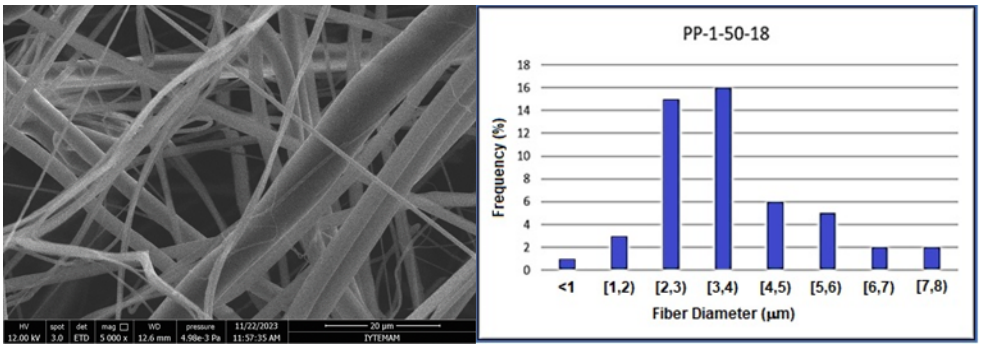
3.1 SEM and Fiber Diameter

Average fiber diameter (AFD) and fiber diameter distribution are essential factors influencing various physical properties of meltblown nonwovens, as they dictate the surface area, which is crucial for numerous applications, including filtration. Figure 3, 4, 5 and 6 indicate the SEM morphologies of micro fibrous nonwovens and their fiber diameter distributions.

CC BY NC ND

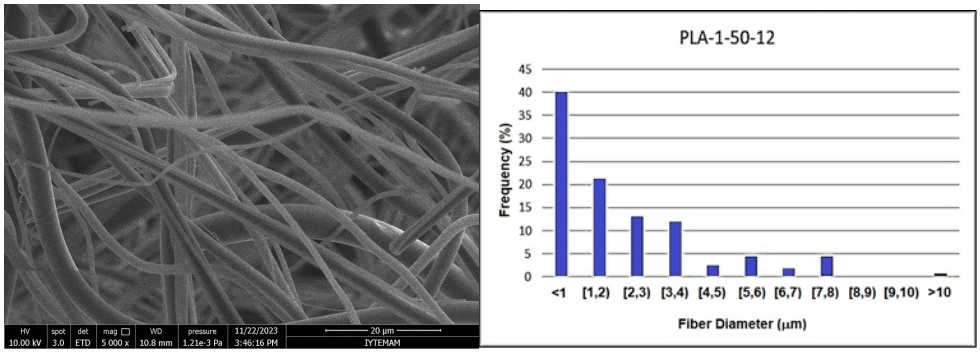


a) b)

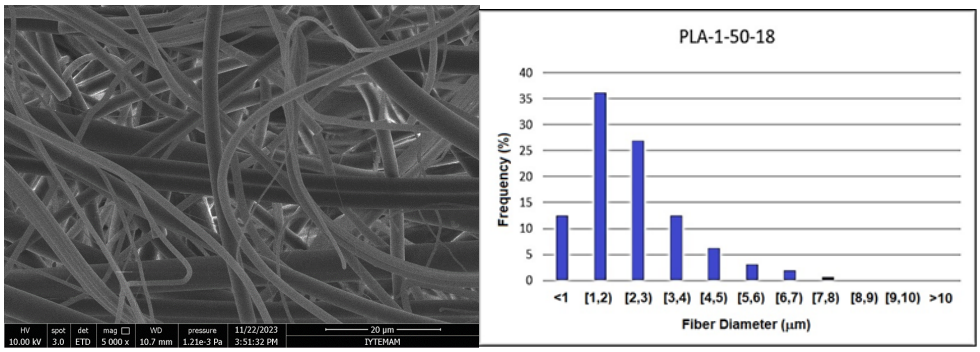


c) d)

Figure 3. SEM images (with 5000 magnification) of a) PP-1-50-12, c) PP-1-50-18 and fiber diameter distributions of b) PP-1-50-12, d) PP-1-50-18 meltblown nonwovens



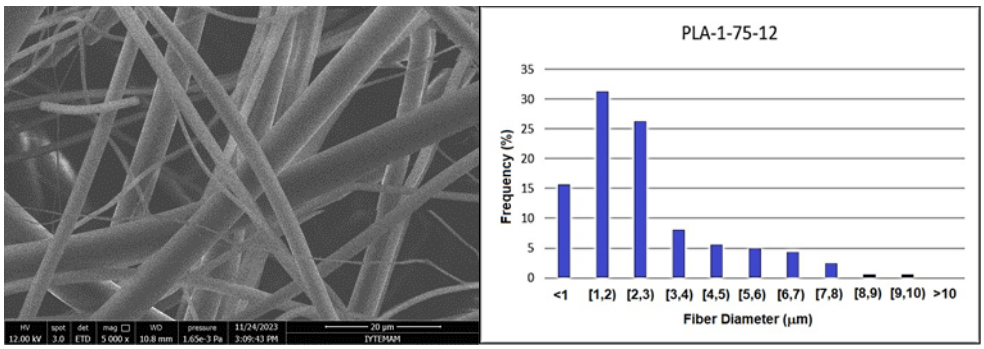
a) b)



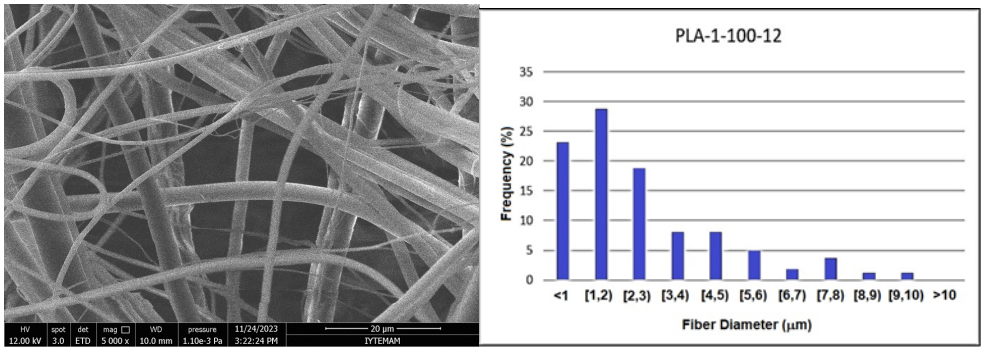
c) d)

Figure 4. SEM images (with 5000 magnification) of a) PLA-1-50-12, c) PLA-1-50-18 and fiber diameter distributions of b) PLA-1-50-12, d) PLA-1-50-18 meltblown nonwovens

BY NC ND

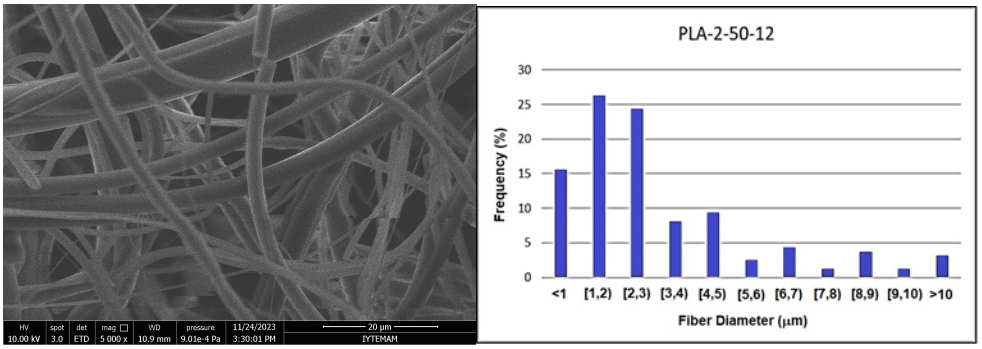


a) b)

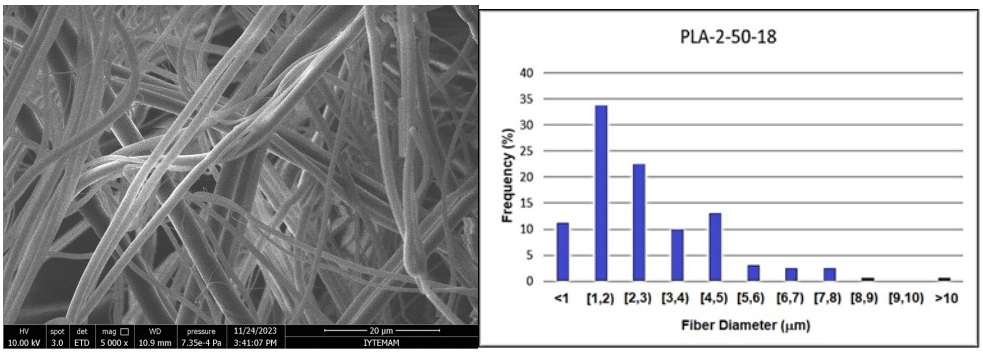


c) d)

Figure 5. SEM images (with 5000 magnification) of a) PLA-1-75-12, c) PLA-1-100-12 and fiber diameter distributions of b) PLA-1-75-12, d) PLA-1-100-12 meltblown nonwovens



a) b)



c) d)

Figure 6. SEM images (with 5000 magnification) of a) PLA-2-50-12, c) PLA-2-50-18 and fiber diameter distributions of b) PLA-2-50-12, d) PLA-2-50-18 meltblown nonwovens

CC BY NC ND

Figure 3, 4, 5 and 6 show that, the PP and PLA micro fibrous nonwovens produced did not exhibit normal fiber diameter distributions but rather asymmetric distributions, which are commonly seen in meltblown structures. Fiber diameter distribution of all samples were positively skewed, which means average diameters are bigger than center value. The frequency of fibers with diameter lover than 1 □m is the highest in sample PLA-1-50-12, produced with 0.18 mm die hole diameter, 50 cm DCD and 12 m/min collector drum speed. At fixed DCD of 50 cm, meltblowns produced with 0.23 mm die hole diameter (PLA-2-50-12 and PLA-2-50-18) exhibited a slightly wider distribution compared to the meltblowns produced with 0.18 mm die hole diameter (PLA-1-50-12 and PLA-1-50-18) for collector drum speeds of both 12 m/min and 18 m/min. An increase in DCD caused broader fiber diameter distribution in PLA meltblowns. At fixed collector drum speed of 12 m/min, die hole diameter of 0.18 mm and air pressure of 8 Psi, PLA-1-75-12 and PLA-1-100-12, produced with 75 cm and 100 cm DCDs respectively, exhibited slightly wider fiber diameter distributions compared to the PLA-1-50-12 produced with 50 cm DCD. Kara and Molnar (24) also mentioned that an increase in DCD leads to fiber collection across a broader area. The effect of collector drum speed on fiber diameter distribution did not show a clear trend in meltblown production.

The average fiber diameter (AFD) of meltblown nonwovens is illustrated in Figure 7.

As shown in figure 7, at a constant air pressure of 8 Psi and a DCD of 50 cm, PLA fibers produced with a die hole diameter of 0.18 mm were thinner than those made with a 0.23 mm die hole diameter. This observation applies to samples collected at both 12 m/min and 18 m/min drum speeds. This result is expected looking at the past studies in the literature which noted that a larger nozzle diameter resulted in thicker fibers (25). Among all the samples the highest AFD was obtained from the PP sample produced with 50 cm DCD, 0.18 mm die hole diameter and 18 m/min collector drum speed, PP-1-50-18, as 3.66 □m. The highest AFD reached by PLA samples was 3.11 □m, achieved by PLA-2-50-1, produced with 50 cm DCD, 0.23 mm die hole diameter and 12 m/min collector drum speed. At constant DCD of 50 cm and 0.18 mm die hole diameter, PP samples exhibited higher AFD values compared to the PLA samples produced with both 12 m/min and 18 m/min collector drum speeds. This variation may stem from differences in melt rheology and solidification characteristics. The previous studies in the literature show that the viscosity in relation to shear rate exhibits distinct behavior for both resins. PLA transitions from a linear viscoelastic state to a shear-thinning behavior as the shear rate rises, whereas PP resin maintains a constant viscosity (4).

Another factor could be the differences in solidification behavior between PP and PLA. The prevailing view is that fiber attenuation occurs due to aerodynamic drag during the meltblowing process. The diameter of meltblown fibers results from the attenuation of the melt stream by the drag force of hot air as the temperature drops rapidly. This drop in air temperature happens within a few centimeters from the die exit. Nevertheless, it has been noted that the fiber diameter continues to change slightly even at greater distances from the die. During the meltblowing process, the fiber diameter may increase due to fiber-to-fiber fusion and disorientation when impacting the collector. As temperatures fall, the viscosity of the polymer melt rises, eventually leading to solidification. This increase in viscosity due to cooling and solidification can impede attenuation and fiber-to-fiber fusion. The smaller fiber diameters observed in PLA meltblown at specific processing conditions are likely a result of the faster solidification of PLA, which limits fiber-to-fiber fusion. In contrast, the PP samples produced with a higher collector drum speed showed a larger fiber diameter, which is likely due to fiber-to-fiber fusion and disorientation upon hitting the collector during melt blowing (4, 15). ANOVA findings with AFD treated as a response variable are presented in Table 3.

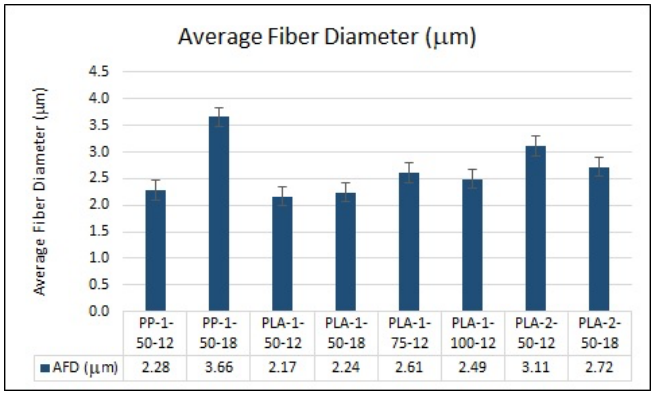


Figure 7. Average fiber diameter (AFD) of meltblown nonwovens

The outcomes of the statistical analysis indicated that die hole diameter had a statistically significant influence on fiber diameters at 95% confidence interval. The results also indicated that the fiber diameter was not significantly influenced by the DCD and collector drum speed in PLA meltblowns.

Table 3. ANOVA findings with AFD treated as a response variable (α=0.05)

	Sum of Squares	df	Mean Square	F	P-Value (Sig.)
Die Hole Diameter	1.926	1	1.926	52.684	0.000
DCD	0.037	2	0.018	0.170	0.845
Collector Drum Speed	0.088	1	0.088	0.863	0.361

CC BY NC ND

These findings are consistent with earlier research. Previous studies indicated that the diameter of the die hole has a substantial effect on the diameters of meltblown fibers, whereas DCD didn't have a statistically significant effect (1). In the literature there are various different reports on the effect of DCD on fiber diameter. Peng et al. (26) observed that a rise in DCD led to an increase in the average diameter of PP meltblowns. Similarly, Lee et al. (27) found that TPU meltblown fiber mats exhibited a continuous increase in fiber diameters as DCD increased. Lee and Wadsworth (28) investigated how processing parameters influenced the melt blowing of PP, noting that a decrease in DCD results in greater fiber entanglement without affecting the average fiber diameter. Choi et al. (29) discovered that increasing DCD diminishes fiber bonding (fusing) while having minimal impact on fiber diameter. Bresee and Qureshi (30) reported that in their study regarding the effect of DCD on the fiber diameter of PP, the average fiber diameter decreased as DCD increased. Jafari et. al. (4) also mentioned that increasing DCD has not significantly decreased the fiber diameter in the production of PLA micro fibrous webs.

3.2 Basis Weight, Thickness and Solidity

Basis weight is one of the factors influencing solidity. Results of basis weight measurements of micro fibrous meltblown nonwovens are presented in Figure 8.

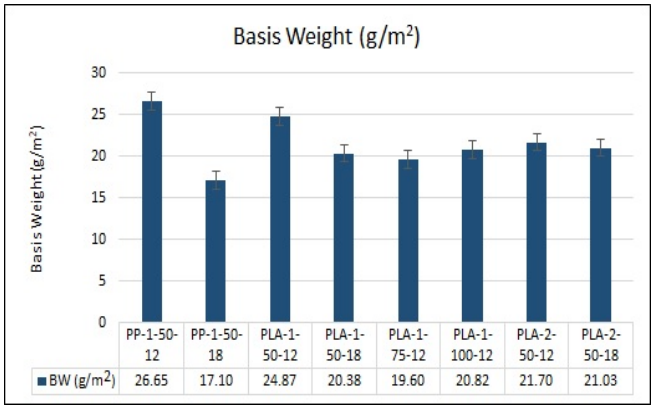


Figure 8. Average basis weight of meltblown nonwovens

ANOVA findings with basis weight treated as a response variable are presented in Table 4. ANOVA findings have shown that die hole diameter, fiber diameter, DCD and collector drum speed had no considerable impact on the basis weight. However, in figure 8, it is evident that for both PP and PLA samples at constant air pressure (8 Psi), DCD (50 cm) and die hole diameter (0.18 mm), the increase in collector drum speed from 12 m/min to 18 m/min caused a decrease in basis weight. This can be explained by lower amount of polymer deposition on the collector drum speed in unit time, at higher speeds. The same trend was valid for the samples prepared using 0.23 mm die hole diameter, even though the difference between the basis weight of the samples prepared with 12 m/min and 18 min are very small. Among the PLA samples, the highest basis weight results were obtained from sample PLA-1-50-12, as 24.87 g/m^2, produced with 0.18 mm die hole diameter, 50 cm DCD, and 12 m/min collector drum speed. Among the PP samples, the highest basis weight results were obtained from sample PP-1-50-12, as 26.65 g/m^2, produced with 0.18 mm die hole diameter, 50 cm DCD, and 12 m/min collector drum speed.

Thickness is another factor influencing solidity. Results of thickness measurements of micro fibrous meltblown nonwovens are shown in Figure 9.

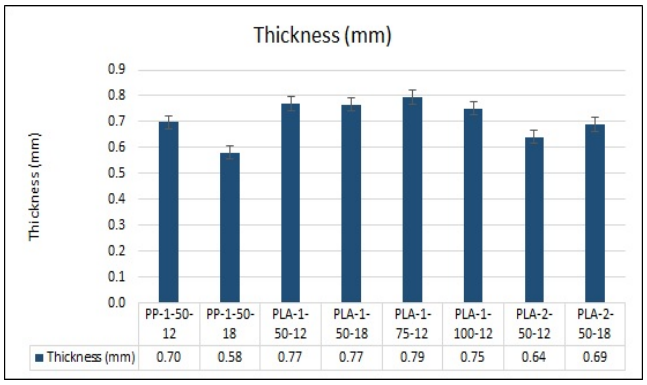


Figure 9. Average thickness of meltblown nonwovens

The outcomes of the statistical analysis indicated that die hole diameter and fiber diameter has a statistically significant influence on thickness, whereas DCD and collector drum speed did not have a statistically significant effect. The ANOVA results while considering thickness as the response variable are presented in Table 5.

Table 4. ANOVA findings with basis weight treated as a response variable (α=0.05)

	Sum of Squares	df	Mean Square	F	P-Value (Sig.)
Die Hole Diameter	0.017	1	0.017	0.001	0.972
DCD	24.986	2	12.493	0.929	0.407
Collector Drum Speed	7.204	1	7.204	0.530	0.473
Fiber Diameter	84.337	5	16.867	1.333	0.284

Table 5. The ANOVA results, with thickness as the response variable (α=0.05)

	Sum of Squares	df	Mean Square	F	P-Value (Sig.)
Die Hole Diameter	0.072	1	0.072	16.989	0.000
DCD	0.027	2	0.014	2.249	0.125
Collector Drum Speed	0.001	1	0.001	0.154	0.698
Fiber Diameter	0.083	5	0.017	3.696	0.013

CC BY NC ND

At given air pressure (8 Psi) and DCD (50 cm), increment in die hole diameter from 0.18 mm to 0.23 mm, caused a decrease in thickness both for the meltblowns produced with 12 m/min and 18 m/min collector drum speeds. The reason for this can be higher fiber diameter and thus less voluminous structure compared to the structures with finer fibers at same basis weight. Even though the results of the statistical analysis have shown that the collector drum speed did not have a statistically significant effect on thickness, it can be seen in figure 9 that in all the samples except from PLA-2-50-18, thickness was reduced by increasing collector drum speed. Just as the basis weight, this can be explained by lower amount of polymer deposition on the collector drum speed in unit time, at higher speeds. PP samples have shown lower thickness values compared to the PLA samples, produced by using the same parameters. This can be explained by larger fiber diameter and less voluminous structure compared to the PLA samples. The highest thickness results were obtained from the sample PLA-1-75-12, produced with 0.18 mm die hole diameter, 75 cm DCD and 12 m/min collector drum speed, as 0.79 mm.

Solidity is one of the most important structural parameters in meltblown nonwovens. In many end uses, such as filtration, desired properties can be achieved by altering the solidity. Air permeability and pressure drop, two significant properties in air filtration, are strongly affected by solidity (4). Average solidity results of micro fibrous meltblown nonwovens are presented in Figure 10.

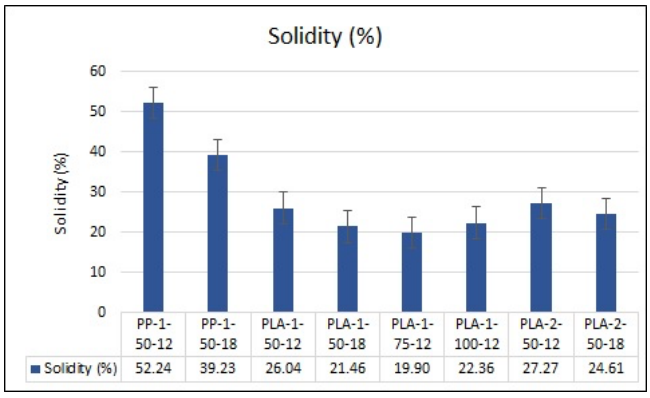


Figure 10. Average solidity of meltblown nonwovens

It can be seen in figure 10 that PP samples have shown higher solidity samples compared to the PLA samples produced with the same production parameters. The high rigidity and elevated glass transition temperature of PLA inhibit excessive bonding between fibers and prevent the structures from collapsing. The highest solidity results were obtained from PP-1-50-12, produced with 0.18 mm die hole diameter, 50 cm DCD and 12 m/min collector drum speed, as 52.24 %.

ANOVA results while considering solidity as a response (α=0.05) are presented in Table 6. The outcomes of the statistical analysis indicated that solidity was significantly influenced by die hole diameter, DCD and fiber diameter. Impact of collector drum speed on solidity was not found significant in statistical means.

Figure 11 illustrates the effect of average fiber diameter (AFD) on the average solidity of meltblown nonwovens.

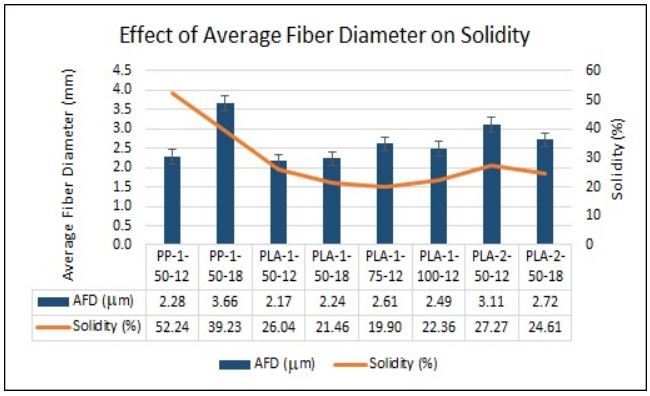


Figure 11. Effect of average fiber diameter (AFD) on average solidity of meltblown nonwovens

Fiber diameter had a significant effect on solidity. Figure 10 and figure 11 shows that, at a constant DCD (50cm), increase in fiber diameter led to a rise in solidity for nonwovens produced at collector drum speeds of both 12 m/min and 18 m/min. Among the PLA samples, higher solidity results were obtained from nonwovens produced with 0.23 mm die hole diameter compared to the ones prepared using 0.18 mm die hole diameters, due to thicker fibers formed. Additionally, the reduced thickness of the samples prepared with the 0.23 mm die hole diameter may also contribute to their higher solidity. The sample PLA-2-50-12 achieved the highest average solidity of 27.27 % among the PLA samples, which was created using a 0.23 mm die hole diameter, a 50 cm DCD, and a collector drum speed of 12 m/min.

The solidity of meltblown nonwovens is strongly affected by DCD. Previous studies have shown that at the given air pressure, an increase in DCD causes a decrease in solidity. (4, 24, 31, 32). In agreement with the previous studies, at a certain air pressure (8 Psi), solidity of micro fibrous webs produced with a 50 cm DCD were greater than that of the samples prepared with a 75 cm DCD, but interestingly solidity of the sample produced with a 100 cm DCD was slightly higher than solidity of the sample produced with 75 cm DCD. This can be explained by higher basis weight and lower thickness of this sample compared to the sample produced with 75 cm DCD.

3.3 Air Permeability

Air permeability is described as the rate at which air flows through the filters due to the pressure difference across the surfaces of the filter web (10). Air permeability

measurement results of meltblown nonwovens are presented in Figure 12.

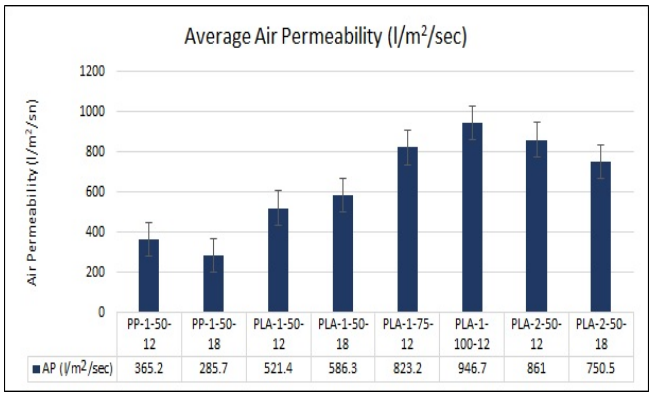


Figure 12. Average air permeability of micro fibrous meltblown nonwovens

Results of statistical analysis have shown that DCD, fiber diameter, solidity and basis weight have significant influence on air permeability in 95% confidence interval. Influence of die hole diameter, collector drum speed and thickness was not found statistically significant. ANOVA results while considering air permeability as a response are presented in Table 7.

Figure 12 shows that, lower air permeability results were obtained from PP samples, compared to PLA samples. This is likely due to the higher basis weight and solidity of PP meltblowns compared to PLA meltblowns. The lowest air permeability results were obtained with PP-1-50-18, produced with 0.18 mm die hole diameter, 50 cm DCD and 18 m/min collector drum speed, as 285.7 l/m^2/sec.

The morphology of filter webs has great effects on air permeability. Also, in previous studies it was explained that fiber diameter has a notable influence on air permeability (10). Figure 13 shows that air permeability of PLA meltblowns increases with increment of AFD, almost linearly at fixed DCD of 50 cm. For example, at fixed DCD of 50 cm, PLA-2-50-12 and PLA-2-50-18 produced with 0.23 mm die hole diameter have higher fiber diameter and thus higher air permeability (861 l/m^2/sec and 750.5 l/m^2/sec) compared to PLA-1-50-12 and PLA-1-50-18 (521.4 l/m^2/sec and 586.3 l/m^2/sec), produced with 0.18 mm die hole diameter respectively. Surprisingly, this was not the case for PP samples. Higher AFD lead to lower air permeability for PP samples in this study.

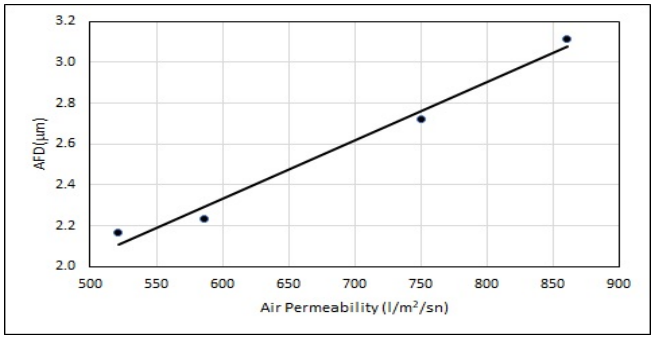


Figure 13. Effect of AFD on air permeability of PLA meltblowns at a constant DCD of 50 cm

On the other hand, solidity is a key factor that influences the air permeability characteristics of meltblown nonwovens. The reduced density enhances the air permeability of PLA meltblowns. This is an advantageous characteristic in air filter materials, since it can lower the pressure drop (4). Figure 14 illustrates that decrement of solidity caused increment in air permeability of PLA meltblowns produced with a 0.18 mm die hole diameter.

It can be seen in Figure 12 and Figure 15 that air permeability of PLA micro fibrous webs increased with increasing DCD. This can be explained by decrement in solidity and the loose structure allowing the passage of more air flow. Previous studies in the has indicated that the decrease in density associated with higher DCD results in greater air permeability in PLA meltblowns (4). Also some studies in the literature explained that increment of DCD results in a softer, fluffier structure, thus increased air permeability (24, 31, 32).

Table 6. The ANOVA findings with solidity treated as a response variable (α=0.05)

	Sum of Squares	df	Mean Square	F	P-Value (Sig.)
Die Hole Diameter	72.600	1	72.600	17.882	0.000
DCD	111.143	2	55.571	19.970	0.000
Collector Drum Speed	2.223	1	2.223	0.338	0.565
Fiber Diameter	186.277	5	37.255	9.45E+31	0.000

Table 7. The ANOVA results while considering air permeability as a response (α=0.05)

	Sum of Squares	df	Mean Square	F	P-Value (Sig.)
Die Hole Diameter	49708.817	1	49708.817	1.060	0.312
DCD	318707.442	2	159353.721	4.123	0.027
Collector Drum Speed	95480.704	1	95480.704	2.111	0.157
Fiber Diameter	677031.142	5	135406.228	4.743	0.004
Solidity	677031.142	5	135406.228	4.743	0.004
Basis Weight	1295090.617	21	61670.982	7.356	0.003
Thickness	537549.992	20	26877.500	0.293	0.989

CC BY NC ND

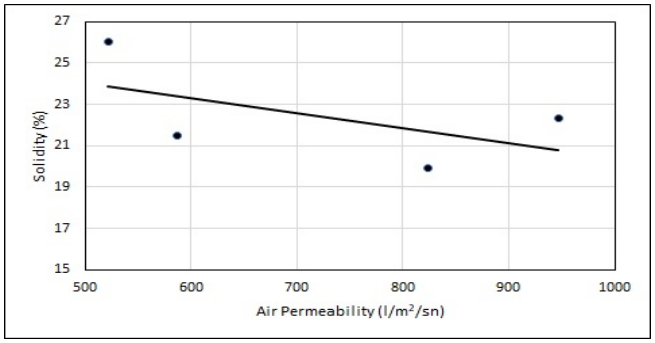


Figure 14. Effect of solidity on air permeability of PLA meltblowns at a die hole diameter of 0.18 mm

With a constant collector drum speed of 12 m/min and a die hole diameter of 0.18 mm, air permeability rose as DCD increased. The peak air permeability values were achieved with PLA-1-100-12 (946.7 l/m²/sec), which was produced using a die hole diameter of 0.18 mm, a collector drum speed of 12 m/min, and a DCD of 100 cm.

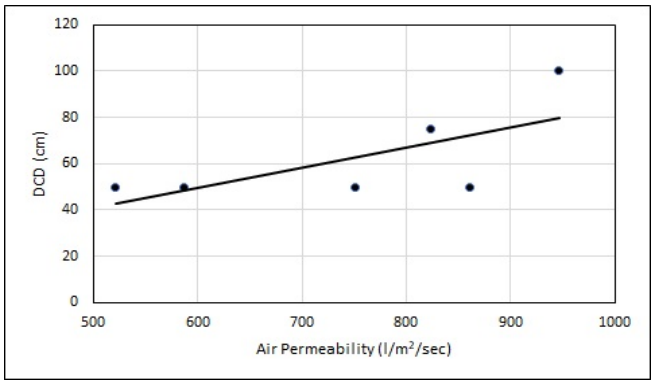


Figure 15. Effect of DCD on air permeability of PLA meltblowns

Fiber diameter distribution can also influence air permeability. The lowest air permeability results were recorded for PLA-1-50-12 (521.4 l/m²/sec), produced with a 0.18 mm die hole diameter, a 12 m/min collector drum speed and a 50 cm DCD. PLA-1-50-12 had the lowest AFD and larger amount of fibers thinner than 1 µm, compared to other samples.

3.4 Water Contact Angle (WCA)

The average water contact angle (WCA) of micro fibrous meltblown nonwovens are presented in Figure 16. Meltblowns nonwovens produced in this study exhibited hydrophobic characteristics, with average contact angles ranging from 93.13 to 137.34. Higher water contact angles were obtained with PP samples, compared to PLA samples.

Figure 17 illustrates the impact of DCD on water contact angle of PLA meltblowns. Decrement in DCD caused a decrement in contact angle, due to increased solidity. For example, decrease of DCD from 75 cm to 50 cm caused a decrease of 19,61 in the contact angle. Among all the samples, the highest contact angle results were obtained with PLA-1-75-12 (118.97) and PLA-1-100-12 (112.24), produced with 75 cm and 100 cm DCD respectively. The lowest contact angle result was obtained with PLA-1-50-12 (93.13 °), produced with 0.18 mm die hole diameter, 12 m/min collector drum speed and 50 cm DCD. At the same time this is the sample with highest basis weight and lowest AFD.

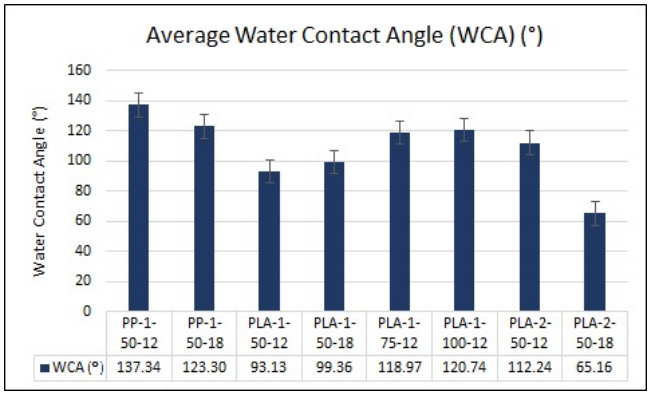


Figure 16. Average water contact angle (WCA) of meltblown nonwovens

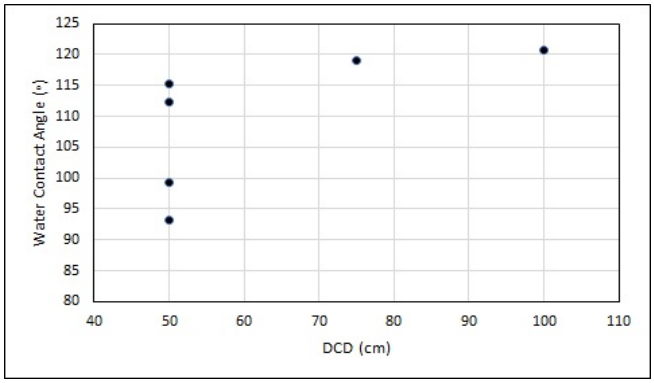


Figure 17. Effect of DCD on water contact angle of PLA meltblown nonwovens

Figure 18 illustrates the influence of average fiber diameter (AFD) on the water contact angle of PLA meltblowns, using a constant die hole diameter of 0.18 mm. The contact angle showed a nearly linear increase with larger fiber diameters.

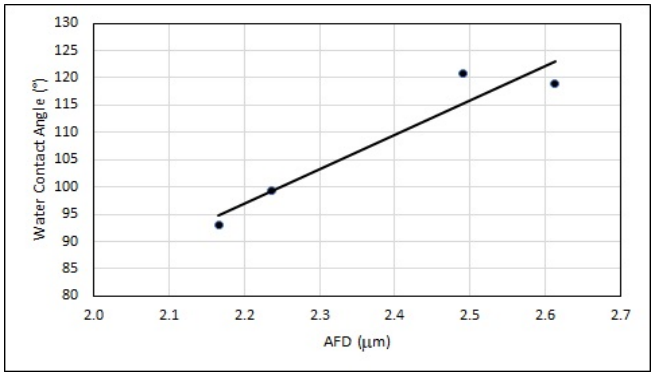


Figure 18. Effect of AFD on water contact angle of PLA meltblowns at fixed die hole diameter of 0.18 mm

The contact angle reduced as solidity and basis weight increased. Figure 19 shows the solidity's effect on water contact angle of PLA meltblowns at fixed die hole diameter (0.18 mm). Thickness did not appear to have a statistically

significant effect on water contact angle at 95% confidence interval.

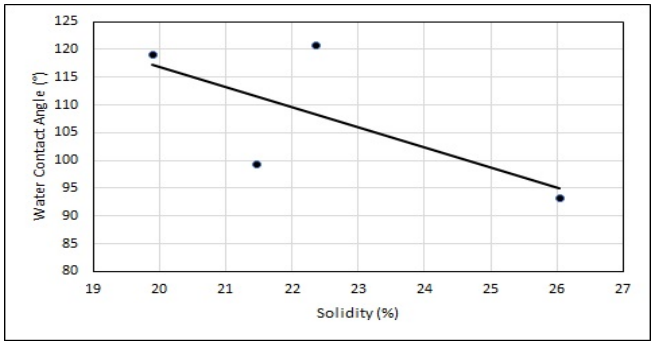


Figure 19. Effect of solidity on water contact angle of PLA meltblowns at fixed die hole diameter of 0.18 mm

ANOVA results while considering water contact angle (WCA) as a response are presented in Table 8. It can also be seen in Table 8 that DCD, fiber diameter, solidity and basis weight has a statistically significant effect on water contact angle, whereas die hole diameter, collector drum speed and thickness did not have a statistically significant effect in 95 % confidence interval.

3.5 Particle Filtration

The structure of the filter material, including fiber diameter, density, and thickness, influences the mechanical efficiency of aerosol filtration and the pressure drop across the filter (4). The parameters of the meltblowing process and the properties of the polymer have an impact on the filter structure, which in turn affects its filtration performance. Average pressure drop and particle capture efficiency of meltblown nonwovens are presented in Figure 20. Figure 20 shows that, among the samples produced from PLA, PLA-2-50-18 achieved the highest filtration efficiency at 57.98%, accompanied by the greatest pressure drop of 75 Pa. Samples produced from PP exhibited higher filtration efficiency and also higher pressure drop compared to the samples produced from PLA. The highest filtration efficiency (71.48%) and pressure drop (130 Pa) was obtained from PP-1-50-18. The higher filtration efficiency of the samples produced with PP can be axplained by higher solidity and basis weight of PP samples. But it should also be considered that PP samples showed gerater pressure drop values compared to PLA samples. Looking at the past studies, there are higher results in air filtration efficiency; such as 90% or more, but these results are mostly obtained with electret filters. Considering that PLA and PP meltblowns investigated in this study are as-produced (not electrostatically charged), the results align with the existing literature. Pu et. al. (33) compared the particle filtration efficiencies of electrostatic assisted PP meltblowns with conventional meltblowns and mentioned that they obtained a filtration efficiency of 40.45 % with conventional meltblowns for 0.3 µm particle size. Jafari et. al (4) produced PLA electret filters by using Reicofil meltblown process and compared their filtration efficiencies with PP meltblown for 0.3 µm monodisperse DOP (dioctyl phthalate) particles reporting that filtration efficiency of uncharged PLA meltblowns were between 15-41%.

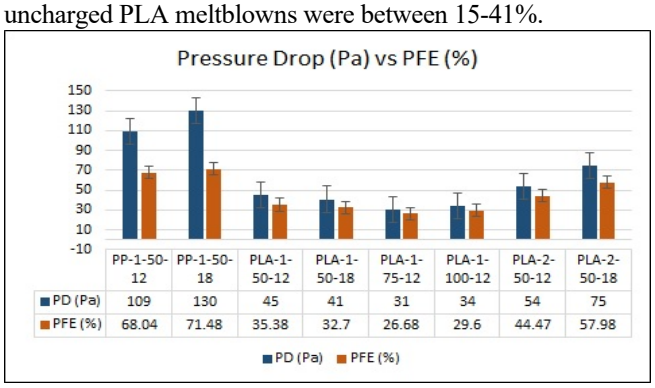


Figure 20. Pressure drop and particle capture efficiency of meltblown nonwovens

Results of statistical analysis (Table 9) in our study have shown that die hole diameter, DCD, collector drum speed, fiber diameter, basis weight and solidity had significant influence of particle filtration efficiency (PFE) and pressure drop at 95% confidence interval, whereas The impact of thickness was not statistically significant. As illustrated in Figure 20, filtration efficieny and pressure drop of PLA meltblowns followed the same trend. PLA meltblowns produced with 0.23 mm die hole diameter namely; PLA-2-50-12 and PLA-2-50-18 showed higher filtration efficiencies 44.47% and 57.98% respectively, compared to the meltblowns produced with 0.18 mm die hole diameter; PLA-1-50-12 and PLA-1-50-18 with 35.38% and 32.7% filtration efficiencies respectively. This is an interesting result since the average fiber diameters of PLA-2-50-12 and PLA-2-50-18 are higher than PLA-1-50-12 and PLA-1-50-18. This can be one reason of The meltblowns with thinner fibers are expected to exhibit higher filtration efficiencies due to enlarged area. But fiber diameter is not the only factor affecting the filtration efficiency. Filtration efficiency is also effected by solidity. Solity values of PLA-2-50-12 and PLA-2-50-18 are higher than PLA-1-50-12 and PLA-1-50-18. This can be one reason of this result. Another reason can be that the difference between the fiber diameters did not appear to be so big.

Table 8. The ANOVA results while considering water contact angle (WCA) as a response (α=0.05)

	Sum of Squares	df	Mean Square	F	P-Value (Sig.)
Die Hole Diameter	219.192	1	219.192	1.818	0.188
DCD	1468.746	2	734.373	9.326	0.001
Collector Drum Speed	106.880	1	106.880	0.858	0.362
Fiber Diameter	3116.948	5	623.390	31.301	0.000
Solidity	3116.948	5	623.390	31.301	0.000
Basis Weight	3507.167	21	167.008	15.224	0.000
Thickness	2422.415	20	121.121	0.930	0.579

CC BY NC ND

Fiber diameter distribution is also an important factor influencing the air filtration efficiency. Previous studies in the literature mentioned that, a broader or bimodal fiber distribution may advantage air filtration by enhancing compression resistance and increasing the filter's thickness. In contrast, for liquid filtration, a narrow distribution of fiber diameters is preferred, as uniform pore sizes are essential because straining is the most important mechanism for capturing particles in liquid filtration (4). PLA-2-50-12 and PLA-2-50-18 showed slightly wider fiber diameter distributions compared to PLA-1-50-12 and PLA-1-50-18 respectively.

The pressure drop and air permeability are key determinants of the breathability properties (10). ANOVA results while considering pressure drop as a response are presented in Table 10. Table 10 shows that die hole diameter, DCD, collector drum speed and basis weight had a statistically significant effect on pressure drop, whereas thickness didn't have a statistically significant effect. The results are in accordance with particle filtration efficiency (PFE).

PLA-1-50-12 and PLA-1-50-18 showed reduced pressure drop characteristics compared to PLA-2-50-12 and PLA-2-50-18, due to higher solidity.

DCD has a remarkable effect on pressure drop. The research results have shown that pressure drop decreased with increasing DCD, since higher DCD leads to a fluffier structure, reduced solidity and thus higher air permeability. At fixed die hole diameter (0.18 mm) and collector drum speed (12 m/min), meltblowns produced with 75 cm (PLA-1-75-12) and 100 cm DCD (PLA-1-100-12) showed lower pressure drop results (31 Pa and 34 Pa respectively) compared to PLA-1-50-12 (45 Pa), produced with 50 cm DCD.

Figure 21 shows the effect of solidity on PFE. It can clearly be seen that at fixed collector drum speed of 12 m/min, filtration efficiency increases with increment in solidity.

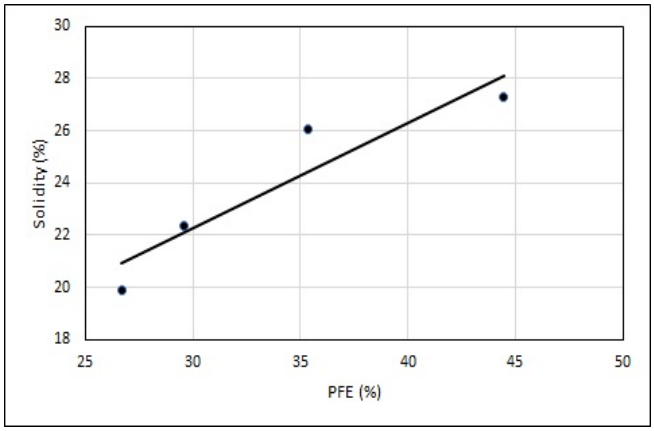


Figure 21. Effect of Solidity on particle filtration efficiency of PLA nonwovens at fixed collector drum speed of 12 m/min

Figure 22 shows the effect of DCD on filtration efficiency at fixed drum speed of 12 m/min. Filtration efficiency decreased with increasing DCD. The reason of the decrement of filtration efficiency with increment of DCD is decrement in solidity and a fluffier, loose structure.

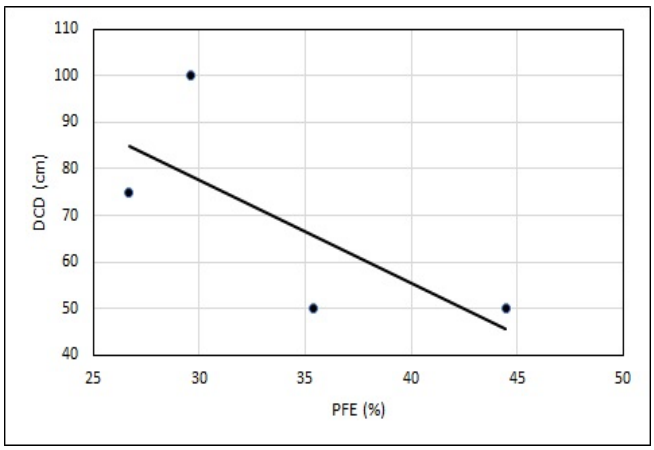


Figure 22. Effect of DCD on particle filtration efficiency of PLA nonwovens at fixed collector drum speed of 12 m/min

Table 9. The ANOVA findings, which focus on particle filtration efficiency (PFE) as a re-sponse variable (α=0.05)

	Sum of Squares	Df	Mean Square	F	P-Value (Sig.)
Die Hole Diameter	2702.788	1	2702.788	113.016	0.000
DCD	1421.533	2	710.767	9.837	0.001
Collector Drum Speed	852.397	1	852.397	9.471	0.005
Fiber Diameter	3372.410	5	674.482	8.55E+32	0.000
Solidity	3372.410	5	674.482	8.6E+32	0.000
Basis Weight	3281.150	21	156.245	13.697	0.000
Thickness	2487.686	20	124.384	1.265	0.371

Table 10. The ANOVA results while considering pressure drop as a response (α=0.05)

	Sum of Squares	df	Mean Square	F	P-Value (Sig.)
Die Hole Diameter	4770.417	1	4770.417	77.828	0.000
DCD	3032.917	2	1516.458	11.855	0.000
Collector Drum Speed	1926.667	1	1926.667	11.830	0.002
Basis Weight	6266.167	21	298.389	10.826	0.001
Thickness	4767.417	20	238.371	1.248	0.380

Figure 23 shows the effect of air permeability on particle filtration efficiency of PLA nonwovens atproduced with 0.18 mm die hole diameter. Filtration efficiency decreases with increasing air permeability.

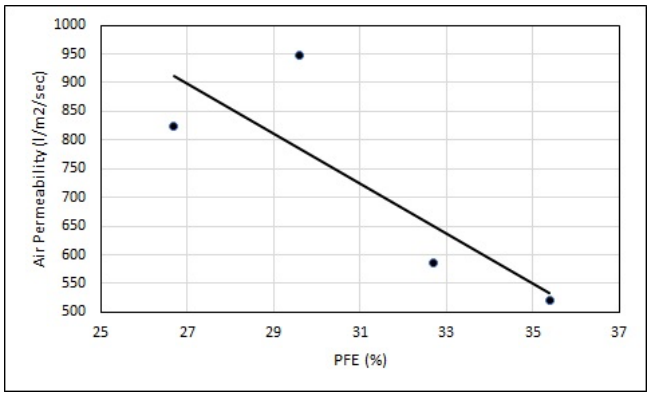


Figure 23. Effect of air permeability on particle filtration efficiency of PLA meltblowns produced with 0.18 mm die hole diameter

Figure 24 shows the influence of basis weight on particle filtration efficiency of PLA meltblowns produced with 0.18 mm die hole diameter. Filtration efficiency increased with increasing basis weight, due to increased solidity and denser structure of the media and thus higher amount of particles captured.

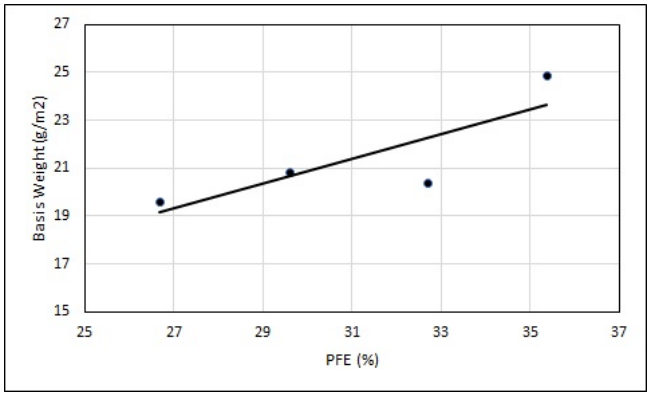
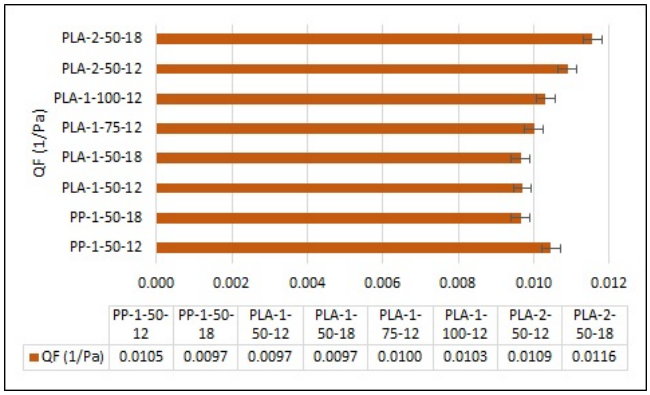


Figure 24. The influence of basis weight on particle filtration efficiency of PLA nonwovens produced with 0.18 mm die hole diameter

The effectiveness of filter media is represented by the quality factor (QF), which integrates both filtration efficiency and pressure drop (10). The QF results for all samples are presented visually in Figure 25.

Figure 25 shows that samples produced with PLA exhibited higher QF values compared to the samples produced with PP, with the same production parameters. The reduced solidity of the samples made from PLA enhanced filtration performance by increasing air permeability and decreasing pressure drop. This lower pressure drop in PLA meltblown nonwovens results in higher quality factors compared to those of PP meltblown nonwovens. Considering the results, the dominant factor effecting the QF of PLA meltblown investigated in this study appears to be the solidity. The highest QF results were obtained with PLA samples produced by using 0.23 mm die hole diameter and 50 cm DCD. The calculated results indicate that the PLA-2-50-12 and PLA-2-50-18 microfiber webs exhibited quality factors (QF) of 0.0116 Pa^{-1} and 0.0109 Pa^{-1}, respectively, outperforming several previously studied bio-based microfiber and nanofiber filters (4, 10).



	PP-1-50-12	PP-1-50-18	PLA-1-50-12	PLA-1-50-18	PLA-1-75-12	PLA-1-100-12	PLA-2-50-12	PLA-2-50-18
QF (1/Pa)	0.0105	0.0097	0.0097	0.0097	0.0100	0.0103	0.0109	0.0116

Figure 25. The quality factor (QF) of meltblown nonwovens

Filtration performance results of various studies about PLA and PP filtersexisting in the literature are presented in table 11. In many studies in the literature, mixed techniques or some treatments such as Corona charging were used in combination with meltblowing. to enhance filtration efficiency. Over 90% filtration performances were obtained in such studies (4, 34, 35, 36, 37, 38). But when the results of the as produced materials (not charged) in the literature performances of those meltblown filters are considered, it can be seen that higher filtration efficiency was obtained in this manuscript (4, 33, 37). In the future, various production or finishing techniques could be explored alongside melt blowing as a continuation of this research.

4. CONCLUSION

Polylactic acid (PLA) nonwovens were effectively produced under suitable processing conditions using two dies with varying die hole diameters. 2 polypropylene (PP) samples were also produced by using the same production parameters for comparison. The properties of the PLA nonwovens dependent on the processing parameters such as die hole diameter, collector drum speed and DCD properties were investigated. The average fiber diameter (AFD) of PLA meltblowns ranged between 2.17-3.11 micrometers. This range was 2.28-3.66 for PP meltblowns. The difference between the fiber diameters is likely to be caused by the rheological and solidification differences between PLA and PP polymers. The air permeability increased as the average fiber diameter (AFD) and DCD increased, but decreased as the solidity decreased. The PLA and PP meltblowns produced in this study exhibited hydrophobic properties with an average contact angle ranging between 93.13°- 120.74° for PLA and 123.30°-134.37° for PP. The water contact angle of PLA meltblowns decreased with decreasing DCD and AFD, but increased with increasing solidity and basis weight. Air filtration efficiency of PLA meltblowns increased with

increasing solidity and basis weight, while it decreased as solidity diminished. Pressure drop decreased with increasing DCD due to reduced solidity and thus higher air permeability. The PLA-2-50-18 achieved the highest filtration efficiency of 57.98%, but also had the highest pressure drop of 75 Pa. The samples produced with PP exhibited higher filtration efficiency values, but also higher pressure drop values compared to the samples produced with PLA. Lower pressure drop of PLA meltblowns lead to higher quality factors than those of PP meltblowns. The effectiveness of filter media is assessed by the quality factor (QF), which considers both filtration efficiency and pressure drop. The dominant factor effecting the QF of PLA meltblown investigated in this study appears to be the solidity. The reduced solidity of the PLA samples enhanced filtration performance by increasing air permeability and decreasing the pressure drop. The calculated results reveal that the PLA-2-50-12 and PLA-2-50-18 microfiber webs exhibited quality factors (QF) of 0.0116 Pa^{-1} and 0.0109 Pa^{-1}, respectively, outperforming several earlier studies on bio-based microfiber and nanofiber filters. The results are consistent with the literature, considering that the PLA meltblowns investigated in this study were as-produced (without electrostatic charging); their filtration performance and biodegradability characteristics make them promising candidates, as sustainable nonwovens, for air filtration applications and other applications such as battery separation and water treatment. The development of sustainable filters made from bioplastics is closely aligned with numerous United Nations Sustainable Development Goals (39).

Abbreviations

The following abbreviations are used in this manuscript:

DCD	Die to collector distance
DEHS	Di-ethyl-hexyl-sebacat
PLA	Poly lactic acid
HVAC	Heating, ventilating and air conditioning
PP	Polypropylene
PE	Polyethylene
PET	Poly (ethylene terephthalate)
PBT	Poly (butylene terephthalate)
PUR	Polyurethane
PA	Polyamide
A-HNT	Aminated halloysite nanotubes
St-co-GMA	Glycidyl methacrylate-styrene
DOP	Dioctyl phthalate
AFD	Average fiber diameter
WCA	Water contact angle
SEM	Scanning electron microscope
ANOVA	Analysis of variance
QF	Quality factor
TPU	Thermoplastic polyurethane
PFE	Particle filtration efficiency

Table 11. Filtration performance results of various studies about PLA and PP filters existing in the literature.

Filter Material	Filter Production method	Filtered Particle	Filtration efficiency (%)	Pressure Drop (Pa)	Quality Factor (Pa^{-1})	Reference
PLA, PP	Meltblowing+ Corona Charging	0.3 µm monodisperse DOP	PLA (Charged):93.2 PP (Charged):88.6 PLA (Not Charged): 40-50 PP (Not Charged): 40	PLA (Charged):38.2 PP (Charged):55.9 PLA (Not Charged): 40-50 PP (Not Charged): 40	PLA (Charged):0.08-0.09 PP (Charged):0.03 PLA (Not Charged): 0.01-0.02 PP (Not Charged): 0-0.01	Jafari et.al. (2021) (4)
PP	Electrostatic-Assisted Meltblowing	0.3 µm DEHS	Charged: 50.83 Not Charged: 40.65			Pu et.al. (2018) (33)
PP	Meltblowing+ Corona Charging	0.26 µm NaCl	98.46	60.7		Liu et.al. (2020) (34)
PP	Meltblowing+ Corona Charging	0.3 µm NaCl	>96	38		Cheng et. al. (2021) (35)
PP+ magnesium stearate	Meltblowing+ Corona Charging	0.3 µm NaCl	99.03	82.32	0.056	Zhang et. al. (2021) (36)
PLA	Meltblowing	0.3 µm NaCl	48.5-54	1-2 mmH_2O/mm		S. Kalani et. al. (2025) (37)
PLA	Meltblowing + Breath Figure	2.5 µm NaCl	Meltblown: 59.5 Meltblown+Breath Figure: 95.8	Meltblown+Breath Figure: 39.3		Zhao et. al. (2025) (38)
PLA, PP	Meltblowing	0.3 µm NaCl	PLA:57.98 PP:71.48	PLA:75 PP:130	PLA:0.0166 PP:0.0105	Our Manuscript

CC BY NC ND

REFERENCES

1. Duran K, Duran D, Oymak G, Kılıç K, Öncü E, Kara M. 2013. Investigation of the physical properties of meltblown nonwovens for air filtration. *Tekstil ve Konfeksiyon* 23(2), 136-142.
2. Bresee RR, Qureshi UA. 2004. Influence of processing conditions on melt blown web structure: Part 1 – DCD. *Journal of Engineered Fibers and Fabrics* 13(1), 49-55.
3. Duran D, Perincek S. 2010. The effect of various production parameters on the physical properties of polypropylene meltblown nonwovens. *Industria Textila* 61(3), 117-123.
4. Jafari M, ShimE, JoijodeA. 2021. Fabrication of poly(lactic acid) filter media via the meltblowing process and their filtration performances: A comparative study with polypropylene meltblown. *Separation and Purification Technology* 260, 118185.
5. Liu G, Guan J, Wang X, Yu J, Ding B. 2023. Polylactic acid (pla) melt-blown nonwovens with superior mechanical properties. *ACS Sustainable Chemistry and Engineering* 11(10), 4279-4288.
6. Yu B, Han J, Sun H, Zhu F, Zhang Q, Kong J. 2015. The preparation and property of poly(lactic acid)/tourmaline blends and melt-blown nonwoven. *Polymer Composites* 36(2). 264–271.
7. Zhang D, Sun C, Beard J, Brown H, Carson I, Hwo C. 2002. Development and characterization of poly(trimethylene terephthalate)-based bicomponent meltblown nonwovens. *Journal of Applied Polymer Science* 83, 1280–1287.
8. Drabek J, Zatloukal M. 2019. Influence of long chain branching on fiber diameter distribution for polypropylene nonwovens produced by melt blown process. *Journal of Rheology* 63(4), 519–532.
9. Lee Y, Wadsworth LC. 1990. Structure and filtration properties of melt blown polypropylene webs. *Polymer Engineering and Science* 30(22), 1413–1419.
10. Eticha AK, Akgul Y. 2024. Optimization of gelatin nanofibrous webs fabricated via electrically assisted solution blow spinning for air filtration applications. *International Journal of Environmental Science and Technology* 21, 7135–7152.
11. Khansari S, Sinha-Ray S, Yarin AL, Pourdeyhimi B. 2013. Biopolymer-based nanofiber mats and their mechanical characterization. *Industrial Engineering and Chemistry Research* 52, 15104–15113.
12. Gao D, Wang J, Wang Y, Zhang P. 2016. Effect of melt viscosity on the cell morphology and properties of poly(lactic acid) foams. *Journal of Cellular Plastics* 52(2) 175–187.
13. Duran D, Yılmaz HA. 2019. Investigation of the physical properties of polylactic acid (pla) based meltblown nonwovens for agricultural applications. *Mugla Journal of Science and Technology* 5(2), 97-109.
14. Vink ETH, Rabago R, Glassner DA, Springs B, O'Connor, RP, Jikstadm H, Gruber PR. 2004. The sustainability of NatureWorks polylactide polymers and Ingeo polylactide fibers: an update of the future. *Macromolecular Bioscience* 4(6), 551–564.
15. Hammonds RL, Gazzola WH, Benson RS. 2014. Physical and thermal characterization of polylactic acid meltblown nonwovens. *Journal of Applied Polymer Science* 131(15), 40593.
16. Zhu F, Su J, Zhao Y, Hussain M, Yasin S, Yu B, Han J. 2019. Influence of halloysite nanotubes on poly (lactic acid) melt-blown nonwovens compatibilized by dual-monomer melt-grafted poly (lactic acid). *Textile Research Journal* 89(19-29), 4173-4185.
17. Duran D. 2012. Investigation of the physical characteristics of polypropylene, meltblown nonwovens under varying production parameters. In: A. Z. El Sonbati (Ed.), *Elastomeric polymers*, London, UK: IntechOpen, 243-264.
18. Kilic A, Shim E, Pourdeyhimi B. 2015. Electrostatic capture efficiency enhancement of polypropylene electret filters with barium titanate. *Aerosol Science and Technology* 49(8), 666-673.
19. Tepekiran BN, Calisir MD, Polat Y, Akgul Y, Kilic A. 2019. Centrifugally spun silica (SiO_2) nanofibers for high-temperature air filtration. *Aerosol Science and Technology* 53(8), 921-932.
20. Sipkens TA, Corbin JC, Oldershaw A, Smallwood, GJ. 2022. Particle filtration efficiency measured using sodium chloride and polystyrene latex sphere test methods. *Scientific Data* 9(1), 756.
21. Li W, Shen S, Li H. 2016. Study and optimization of the filtration performance of multi–fiber filter. *Advanced Powder Technology* 27(2), 638–645.
22. Gungor M, Toptas A, Calisir, MD, Kilic A. 2021. Aerosol filtration performance of nanofibrous mats produced via electrically assisted industrial-scale solution blowing. *Polymer Engineering and Science* 61, 2557–2566.
23. Kim HB, Lee WJ, Choi SC, Lee KB, Lee MH. 2021. Filter quality factors of fibrous filters with different fiber diameter *Aerosol Science and Technology* 55(2), 154– 166.
24. Kara Y, Molnár K. 2022. A review of processing strategies to generate melt-blown nano/microfiber mats for high-efficiency filtration applications. *Journal of Industrial Textiles* 51(1_suppl), 137S-180S.
25. Gundogdu NS, Akgul Y, Kilic A. 2018. Optimization of centrifugally spun thermoplastic polyurethane nanofibers for air filtration applications. *Aerosol Science and Technology* 52(5), 515–523.
26. Peng M, Jia H, Jiang L, Zhou Y, Ma J. 2019. Study on structure and property of PP/TPU meltblown nonwovens. *Journal of the Textile Institute* 110(3), 468–475.
27. Lee YE, Wadsworth LC. 2007. Fiber and web formation of melt-blown thermoplastic polyurethane polymers. *Journal of Applied Polymer Science* 105, 3724–3727.
28. Lee Y, Wadsworth LC. 1992. Effects of melt-blowing process conditions on morphological and mechanical properties of polypropylene webs. *Polymer* 33(6), 1200–1209.
29. Choi KJ, Spruiell JE, Fellers JF, Wadsworth LC. 1988. Strength properties of melt blown nonwoven webs. *Polymer Engineering and Science*, 28(2), 81–89.
30. Bresee RR, Qureshi UA. 2006. Influence of process conditions on melt blown web structure. Part IV – fiber diameter. *Journal of Engineered Fibers and Fabrics*, 1(1), 32-46.
31. Xu QY, Wang YM. 2013. The effects of processing parameter on melt-blown filtration materials. *Advanced Materials Research* 650, 78–84.
32. Bresee RR. 2002. Fiber motion near the collector during melt blowing part 1: general considerations. *International Nonwovens Journal* 11, 27–34.
33. Pu Y, Zheng J, Chen F, Long Y, Wu H, Li Q, Yu S, Wang X, Ning X. 2018. Preparation of polypropylene micro and nanofibers by electrostatic-assisted melt blown and their application. *Polymers* 10(9), 959.
34. Liu C, Dai Z, He B, Ke QF. 2020. The Effect of temperature and humidity on the filtration performance of electret melt-blown nonwovens. *Materials* 13, 4774.
35. Cheng S, Muhaiminul ASM, Yue Z, Wang Y, Xiao Y, Militky J, Prasad M, Zhu G. 2021. Effect of temperature on the structure and filtration performance of polypropylene melt-blown nonwovens. *Autex Research Journal* 21(2), 207-217.
36. Zhang X, Liu J, Zhang H, Hou J, Wang Y, Deng C, Huang C, Jin X. 2021. Multi-layered, corona charged melt blown nonwovens as high performance PM0.3 air filters. *Polymers* 13, 485.
37. Kalani S, Jubinville D, Mekonnen TH. 2025. Nano-porous melt-blown poly(lactic acid) fiber mat air filters for high efficiency particulate capture. *Advanced Sustainable Systems 9(3)*, 2400898.
38. Zhao Y, Zhang S, Yan D, Ming J, Wang X, Ning X. 2025. Combination strategy of melt-blowing and breath-figure enabling scale-up production of hierarchically structured polylactic acid (pla) nonwovens for durable and efficient air filtration. *Advanced Fiber Materials* 7, 607-632.
39. United Nations Department of Economic and Social Affairs. 2015. Sustainable Development Goals [Web page]. Retrieved from: https://sdgs.un.org/goals.

CC BY NC ND